SAR interferometry:
A geometrical approach

Laurent Ferro-Famil

SAPHIR team, IETR - UMR CNRS 6164
University of Rennes 1

October 2013

Outline

Elevation mapping using SAR images

Principles of SAR interferometry

Reconstruction of Digital Elevation Models

Progress

Elevation mapping using SAR images
- Principles of SAR imaging
- Space diversity for elevation mapping

Principles of SAR interferometry

Reconstruction of Digital Elevation Models

SAR acquisition geometry

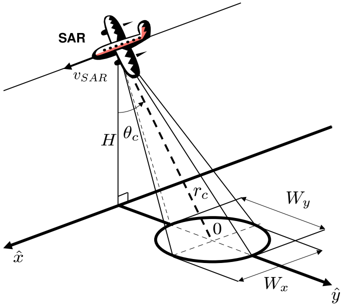

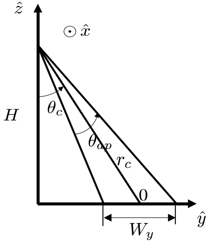

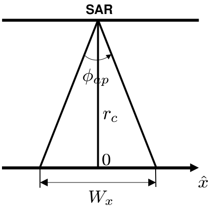

SAR acquisition geometry

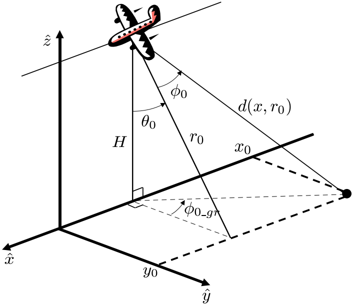

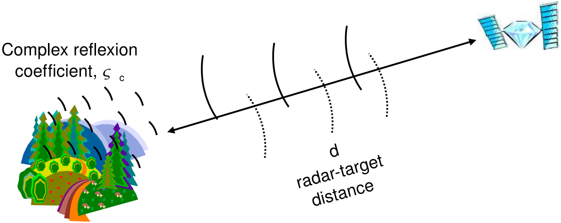

Raw SAR signal

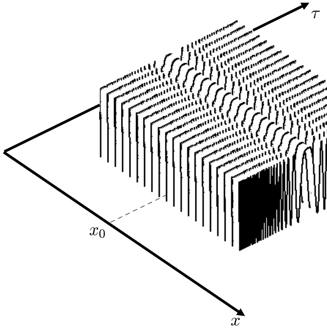

- scatterer located at (x_0, r_0)
- Reflection coefficient a_c
- Baseband lfm signal $p(\tau)\ \mathrm{rect}(\tau/T_p)$

$$
\begin{aligned}
s(x,\tau) = \quad & a_c && \rightarrow \text{complex reflection coefficient} \\
& p(\tau - \tau_0(x))\ \mathrm{rect}\left(\frac{\tau-\tau_0(x)}{T_p}\right) && \rightarrow \text{delayed chirp} \\
& \exp(-j2\pi f_c \tau_0(x)) && \rightarrow \text{delayed carrier phase} \\
& \mathrm{rect}\left(\frac{x-x_0}{W_x}\right) && \rightarrow \text{azimuth aperture}
\end{aligned}
$$

with $\quad \tau_0(x) = 2\frac{\sqrt{r_0^2+(x-x_0)^2}}{c}$ $\quad$ the azimuth varying delay

Range-focused SAR signal

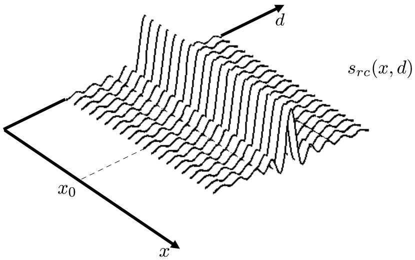

- scatterer located at (x_0, r_0)
- Reflection coefficient a_c
- Range migrations are **neglected**

$$\begin{aligned} s(x,d) = \quad & a_c && \rightarrow \text{complex reflection coefficient} \\ & h_r(d - d_0(x)) && \rightarrow \text{delayed range impulse response} \\ & \exp(-j\tfrac{4\pi}{\lambda_c} d_0(x)) && \rightarrow \text{delayed carrier phase} \\ & \text{rect}\left(\frac{x-x_0}{W_x}\right) && \rightarrow \text{azimuth aperture} \end{aligned}$$

with $d_0(x) = \sqrt{r_0^2 + (x - x_0)^2}$ the azimuth varying radar-scatterer distance

Focused SAR signal

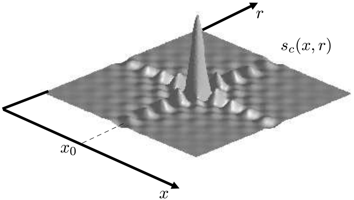

- scatterer located at (x_0, r_0)
- Reflection coefficient a_c
- Range migrations are **neglected**

$$
\begin{aligned}
s(x,r) = \quad & a_c && \rightarrow \textbf{complex reflection coefficient} \\
& h_r(d - r_0) && \rightarrow \text{delayed range impulse response} \\
& h_a(x - x_0) && \rightarrow \text{delayed azimuth impulse response} \\
& \exp(-j\tfrac{4\pi}{\lambda_c} r_0) && \rightarrow \textbf{two-way propagation phase}
\end{aligned}
$$

with $\quad r_0 = d_0(x_0) \quad$ the scatterer position in range

Coherent SAR image

Single Look Complex (SLC) SAR image

- $S(x, r) = A(x, r)\, e^{j\phi(x,r)}$: 2-D array of coherent complex coefficients
- $A \propto |a_c|$ reflection coefficient amplitude, ϕ : absolute phase.

Composite phase information

$$\phi = \phi_r + \phi_{obj} = -\frac{4\pi}{\lambda_c} r + \phi_{obj} = -k_c r + \phi_{obj}$$

- ϕ_r : deterministic component (2-way propagation delay).
- ϕ_{obj} : unknown, may be random.

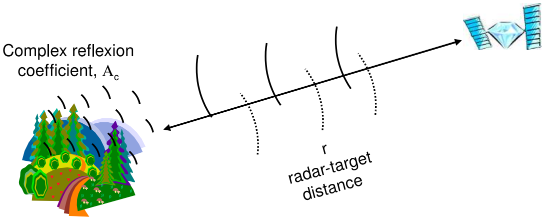

Absolute phase over natural media

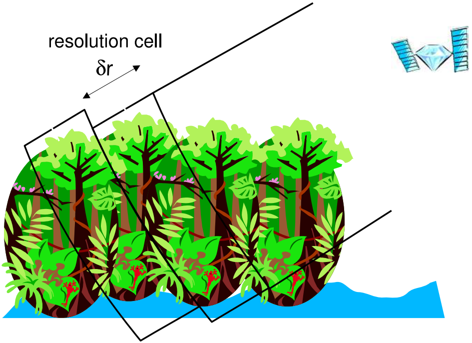

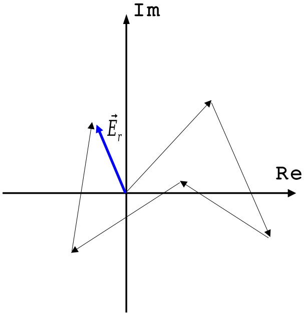

Coherent sum of a **large** number of contributions

- ϕ_{obj} is usually **random**.
- $\phi = \phi_r + \phi_{obj}$ is then **random** too.

Example of a coherent SAR image

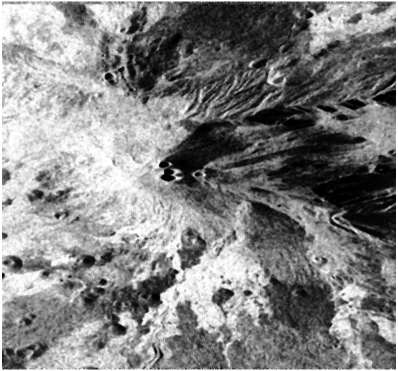

Amplitude image

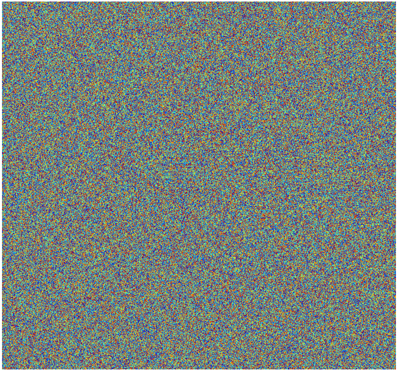

Absolute phase image

SIR-C, X-band, Mount Etna, Italy

Progress

Elevation mapping using SAR images
- Principles of SAR imaging
- Space diversity for elevation mapping

Principles of SAR interferometry

Reconstruction of Digital Elevation Models

Circular ambiguity of SAR imaging

$$\begin{array}{ccccc} \text{3-D reflectivity} & & \text{2-D raw data} & & \text{2-D image} \\ \gamma(x,y,z) & \Rightarrow & s_r(x,\tau) & \Rightarrow & s(x,r) \end{array}$$

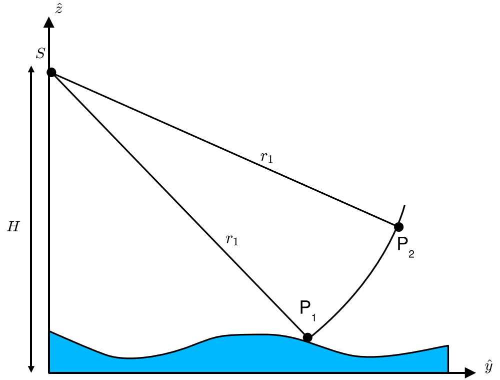

Mapping of $\gamma(x_0, y_0, z_0)$

- good localization in azimuth, x_0 (accuracy : δ_{az})
- circular ambiguity in the $(\hat{y}, \hat{z})$ plane

$$y_i^2 + (H - z_i)^2 = r_0^2$$

$\Rightarrow$ multiple solutions (y_i, z_i)

Solution : two acquisitions with space diversity

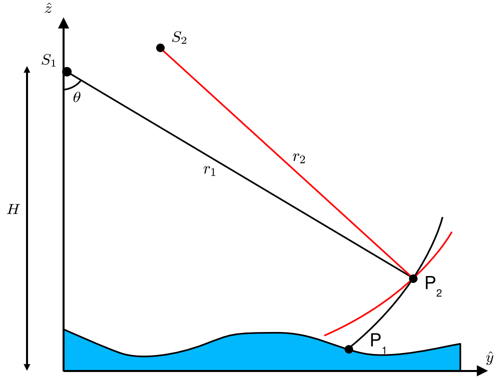

3-step unambiguous estimation

- Slant range distance from S_1

$$r_1 = ||\overrightarrow{S_1 P_2}|| = ||\overrightarrow{S_1 P_1}||$$

- Slant range distance from S_2

$$r_2 = ||\overrightarrow{S_2 P_2}||$$

- h_2 from r_1, r_2 and the geometrical configuration

Geometrical configuration

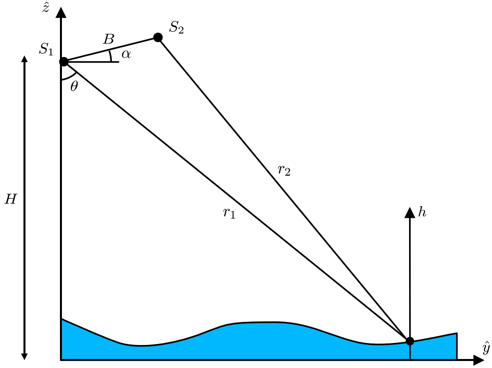

Acquisition geometry descriptors

- $S_{1,2}$: sensor positions
- B : baseline
- α : baseline inclination
- $r_{1,2}$: slant range distances
- h : elevation position
- H : altitude above reference
- θ : off-nadir incidence angle
- y : ground range position

Baseline conventions

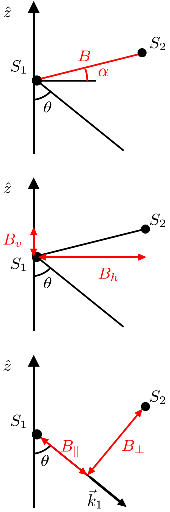

Polar convention

- B : baseline length
- α : baseline inclination

Cartesian convention

- $B_h = B\cos\alpha$: horizontal baseline
- $B_v = B\sin\alpha$: vertical baseline

Wave convention

- $B_\parallel = B\sin(\theta - \alpha)$: baseline parallel to $\vec{k}_1$
- $B_\perp = B\cos(\theta - \alpha)$: baseline perpendicular to $\vec{k}_1$

Measuring range positions with SAR images

Bad limited focused SAR signal

$$
\begin{aligned}
s_i(x,r) = \quad & a_{c_i} \\
& h_r(r - r_i) && \rightarrow \text{located around } r = r_i \\
& h_a(x - x_0) \\
& \exp(-j\tfrac{4\pi}{\lambda_c} r_i) && \rightarrow \text{periodic function of } r_i
\end{aligned}
$$

Incoherent estimation

- Intensity :

$$I_i(x,r) = |s_i(x,r)|^2 \propto |a_{c_i}|^2 |h_r(r - r_i)|^2$$

- Accuracy : range resolution $\delta_r = c/(2B_f)$

Coherent estimation

- Phase :

$$\arg(s_i(x,r)) \propto \arg(a_{c_i}) - \frac{4\pi}{\lambda_c} r_i$$

- Accuracy : ? ?

Incoherent vs. coherent estimation

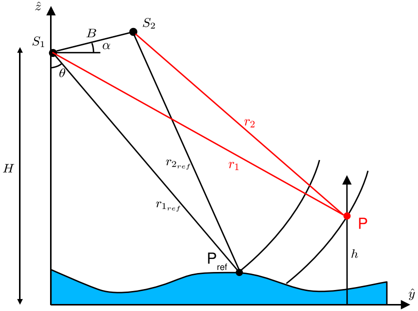

SAR responses

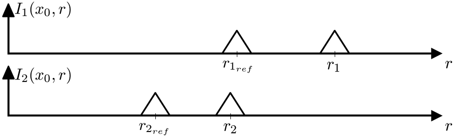

Referencing

- Large shift : $|r_1 - r_2'| > \delta_r$

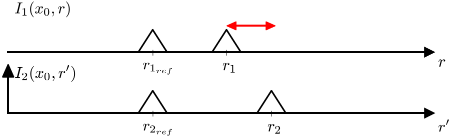

Large B, h, incoherent estimation

- Small shift : $|r_1 - r_2'| < \delta_r$

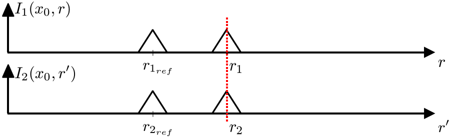

Small B, h, coherent estimation

Radar-grammetry principle

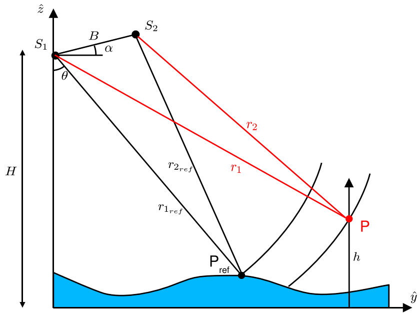

- Find (r_1, r_2) so that

$$I_1(x, r_1) \approx I_2(x, r_2)$$

- Estimate θ from (see appendix)

$$r_2^2 = r_1^2 - 2r_1 B \sin(\theta - \alpha)$$

- Estimate h as

$$h = H - r_1 \cos\theta$$

Incoherent SAR responses

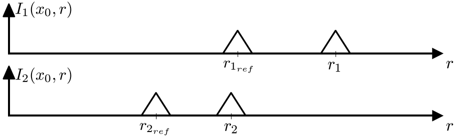

Radar-grammetry accuracy

Estimation accuracy

- Accuracy on r_1, r_2 : range resolution δ_r
- Accuracy on h, several δ_r

Conditions of applications

- B large enough so that $r_1 \neq r_2'$
- h large enough so that $|r_2'(h) - r_2'(0)| > \delta_r$
- Low accuracy method, but robust
- Mainly used for very large scale applications

Example of radar-grammetry application

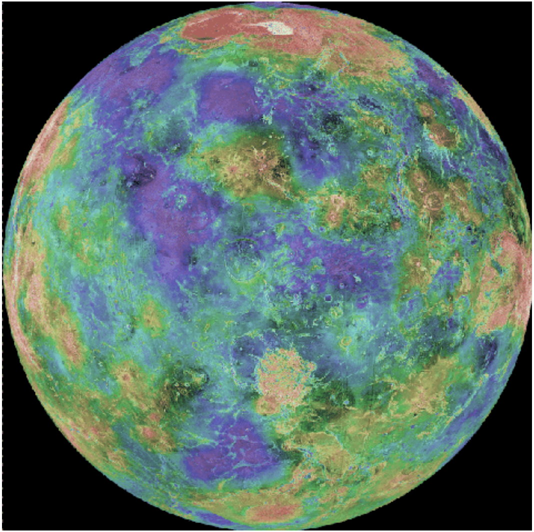

DEM of Venus using SAR data acquired by the Magellan probe

Interferometric information

Coherent SAR responses

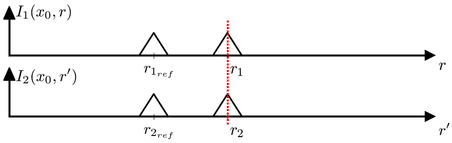

Phase periods within a resolution cell

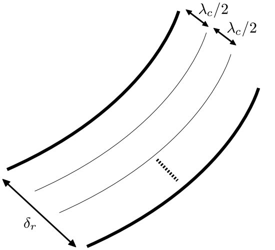

- Coherent information

$$s_1 = |a_{c_1}| \exp\left(-j\frac{4\pi}{\lambda_c} r_1 + j\phi_{obj\,1}\right)$$
$$s_2 = |a_{c_2}| \exp\left(-j\frac{4\pi}{\lambda_c} r_2 + j\phi_{obj\,2}\right)$$

- Assumptions (small baseline)

$$a_{c_1} \approx a_{c_2} \Rightarrow |a_{c_1}| \approx |a_{c_2}|,\ \phi_{obj\,1} \approx \phi_{obj\,2}$$

- Deterministic phase difference

$$\Delta\phi_{12} = \arg(s_1 s_2^*) = -\frac{4\pi}{\lambda_c}\Delta r_{12}$$

- Accuracy
  - $\Delta\phi_{12}$: a fraction of 2π
  - Δr_{12} : a fraction of $\lambda/2$

$\Rightarrow$ very high accuracy on h
$\Rightarrow$ requires small B

Progress

Elevation mapping using SAR images

Principles of SAR interferometry
- Interferometric phase
- Topographic and flat earth components
- Examples of SAR interferometry

Reconstruction of Digital Elevation Models

Interferometric phase : far field approximation

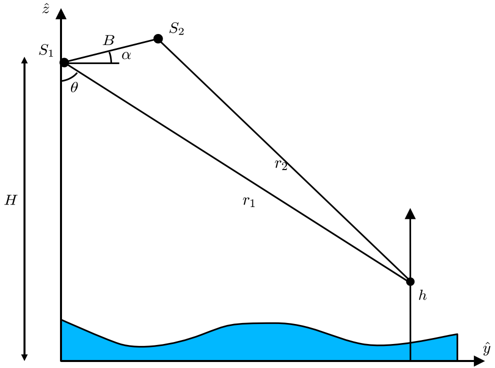

Explicit derivation in the appendix

Far-field approximation

- Condition : $r_1 \gg B$
- $r_2 \approx r_1 - B\sin(\theta - \alpha)$
- $\Delta r_{12} = r_1 - r_2 \approx B\sin(\theta - \alpha)$

Interferometric phase difference

- Modified wavenumber $k_c = 4\pi/\lambda_c$
- Interferometric phase

$$\begin{aligned}\Delta\phi_{12} &= -4\pi/\lambda_c \Delta r_{12}\\ &= k_c B \sin(\alpha - \theta)\end{aligned}$$

- Phase-height dependency

$$\theta = f(h, \dots) \Rightarrow \Delta\phi_{12} = f(h, \dots)$$

Interferometric phase linearization and decomposition

$$\Delta\phi_{12} = k_c B \sin(\alpha - \theta)$$

Interferometric phase sensitive to

- Configuration of acquisition : $k_c,\ B, \alpha$
- Elevation h, range position r_1 : $\theta = \arccos\left(\frac{H-h}{r_1}\right) = f_{nl}(h, r_1)$

Local linearization

- $\mathrm{d}\Delta\phi_{12}(h, r_1) = \frac{\partial \Delta\phi_{12}}{\partial h}\Big|_{r_1} \mathrm{d}h + \frac{\partial \Delta\phi_{12}}{\partial r_1}\Big|_{h} \mathrm{d}r_1$
- Linear approximation valid for small $\Delta h, \Delta r_1$:

$$\Delta\phi_{12}(h+\Delta h, r_1+\Delta r_1) - \Delta\phi_{12}(h, r_1) \approx \frac{\partial \Delta\phi_{12}}{\partial h}\bigg|_{r_1} \Delta h + \frac{\partial \Delta\phi_{12}}{\partial r_1}\bigg|_{h} \Delta r_1$$

- A relative height information may now be estimated from

$$\Delta\Delta\phi_{12} = \Delta\phi_{12}(h+\Delta h, r_1+\Delta r_1) - \Delta\phi_{12}(h, r_1)$$

Interferometric phase linearization and decomposition

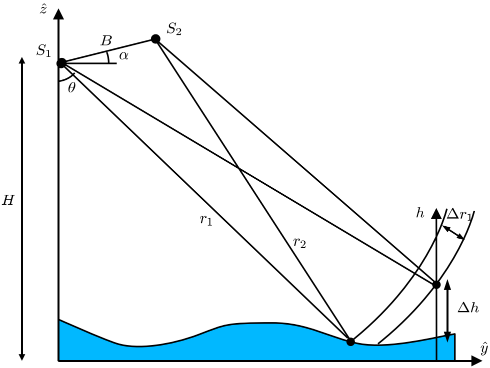

$$\Delta\Delta\phi_{12} \approx \left.\frac{\partial \Delta\phi_{12}}{\partial h}\right|_{r_1} \Delta h + \left.\frac{\partial \Delta\phi_{12}}{\partial r_1}\right|_{h} \Delta r_1$$

Two-term linear decomposition

- "Flat earth" ($\Delta h = 0$) term

$$\Delta\Delta\phi_{fe}(\Delta r_1) = \left.\frac{\partial \Delta\phi_{12}}{\partial r_1}\right|_{h} \Delta r_1$$

- "Topographic" ($\Delta r_1 = 0$) term

$$\Delta\Delta\phi_{topo}(\Delta h) = \left.\frac{\partial \Delta\phi_{12}}{\partial h}\right|_{r_1} \Delta h$$

- Composite interferometric phase

$$\Delta\Delta\phi_{12} = \Delta\Delta\phi_{fe} + \Delta\Delta\phi_{topo}$$

Interferometric phase topographic component

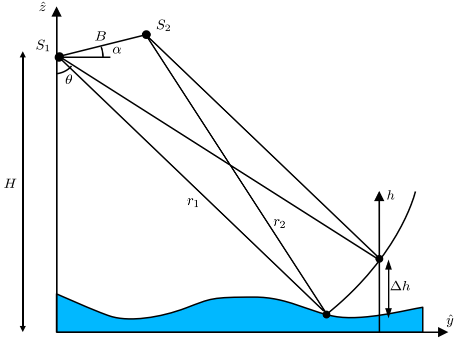

Explicit derivation in the appendix

Topographic phase expression

- Topographic variations ($\Delta r_1 = 0$)

$$\Delta\Delta\phi_{topo} = -\frac{k_c B_\perp}{r_1 \sin\theta}\Delta h$$

Height estimation

$$\Delta h = -\frac{r_1 \sin\theta}{k_c B_\perp}\Delta\Delta\phi_{fe}$$

- Height ambiguity ($0 \leq \Delta\Delta\phi_{topo} \leq 2\pi$)

$$h_{amb} = \frac{2\pi r_1 \sin\theta}{k_c B_\perp}$$

- Phase sensitivity to height

$$\frac{\Delta\Delta\phi_{topo}}{\Delta h} = -\frac{k_c B_\perp}{r_1 \sin\theta}$$

Interferometric phase flat earth component

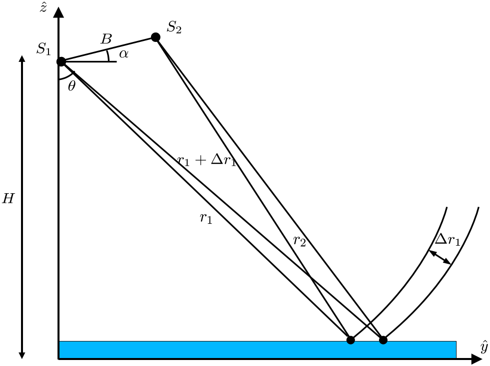

Explicit derivation in the appendix

Flat earth phase expression

- Range variations ($\Delta h = 0$)

$$\Delta\Delta\phi_{fe} = -\frac{k_c B_\perp}{r_1 \tan\theta} \Delta r_1$$

Interferogram flattening

- SAR images $s(x, r)$ with range pixel spacing $d_r \leq \delta_r$
- Computation of flat earth phase

$$\Delta\Delta\phi_{fe} = -\frac{k_c B_\perp}{r_1 \tan\theta} d_r$$

- Interferogram flattening

$$\Delta\Delta\phi_{topo} = \arg e^{j(\Delta\Delta\phi_{12} - \Delta\Delta\phi_{fe})}$$

Interferometric phase measurement : wrapping effect

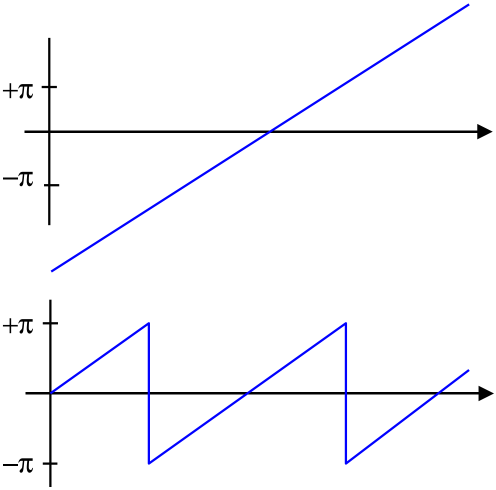

Explicit derivation in the appendix

Interferometric phase computation

- $\Delta\phi_{12} = \arg(s_{12})$, with $s_{12} = s_1 s_2^*$
- Four-quadrant arc-tangent operator

$$\Delta\phi_{12\_est} = \arctan(\Im(S_{12}), \Re(S_{12}))$$

Interferometric phase computation

- $\Delta\phi_{12\_est} \in]-\pi, \pi]$
- $\Delta\phi_{12\_est} = \Delta\phi_{12} + k2\pi,\ k \in \mathbb{Z}$
- Phase wrapping effect : "fringes"

Flat-earth phase fringe frequency

$$f_{fe} = \frac{1}{2\pi}\left|\frac{\partial\Delta\phi_{fe}}{\partial\Delta r}\right| = k_c \frac{B_\perp}{r_1 \tan\theta}$$

Influence of baseline and topography

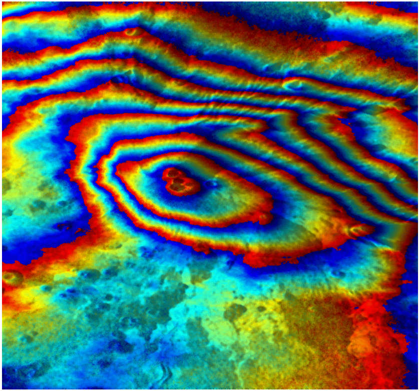

12m baseline

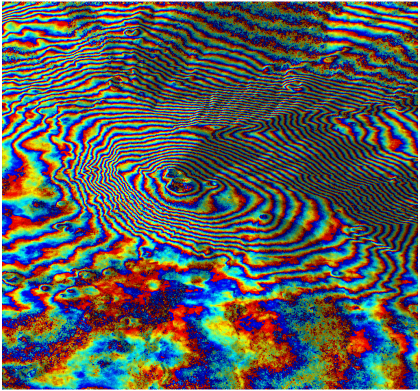

60m baseline

SIR-C, X-band, Mount Etna, Italy

$$\Delta\phi_{topo} = -k_c \frac{B_\perp}{r_1 \sin\theta}\Delta h$$

Influence of flat earth

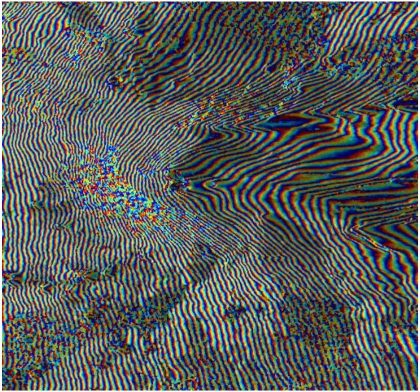

$\Delta\phi_{12}$

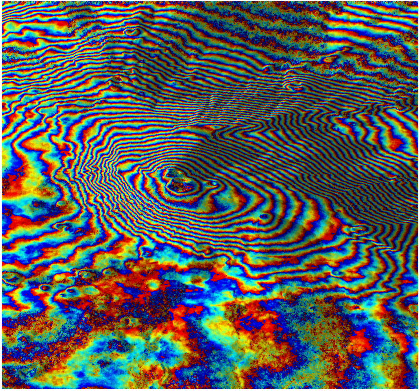

$\Delta\phi_{12} - \Delta\phi_{fe}$

SIR-C, X-band, Mount Etna, Italy

60m baseline

Estimation of the flat earth phase component

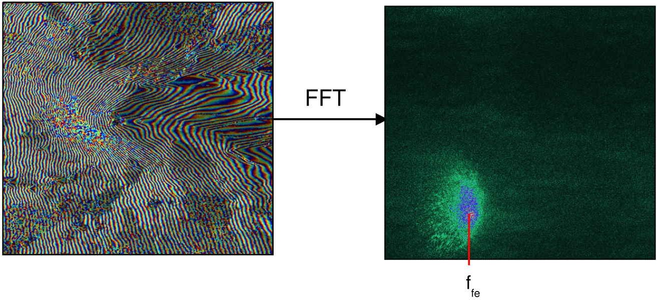

Linear $\Delta\phi_{fe}$ behavior $\Rightarrow$ strong periodic component

Flat earth reconstruction

$$\begin{aligned}\Delta\phi_{fe} &= -k_c \frac{B_\perp}{r_1 \tan\theta}\Delta r \\ &= f_{fe}\Delta r\end{aligned}$$

Flat earth removal

- Erroneous way : $\Delta\phi_{flat} = \Delta\phi_{12} - \Delta\phi_{fe}$
- Correct way : $\Delta\phi_{flat} = \arg\left(e^{j(\Delta\phi_{12} - \Delta\phi_{fe})}\right)$

Influence of the carrier wavelength : amplitude

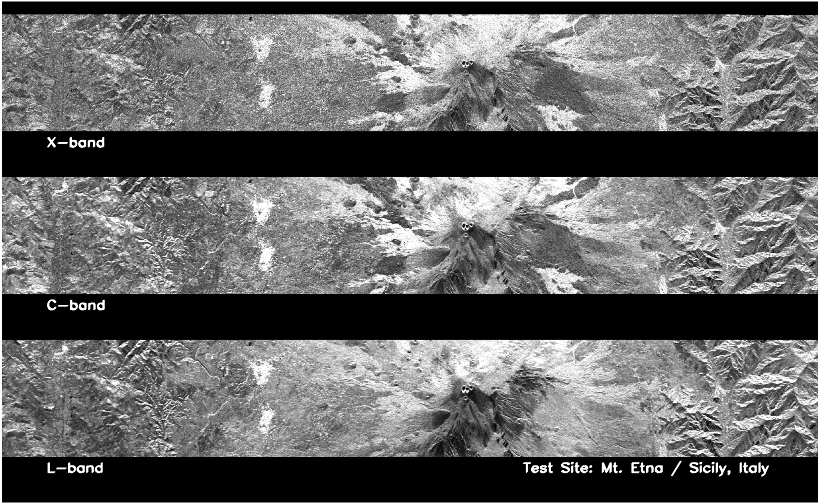

Influence of the carrier wavelength : interferometric phase

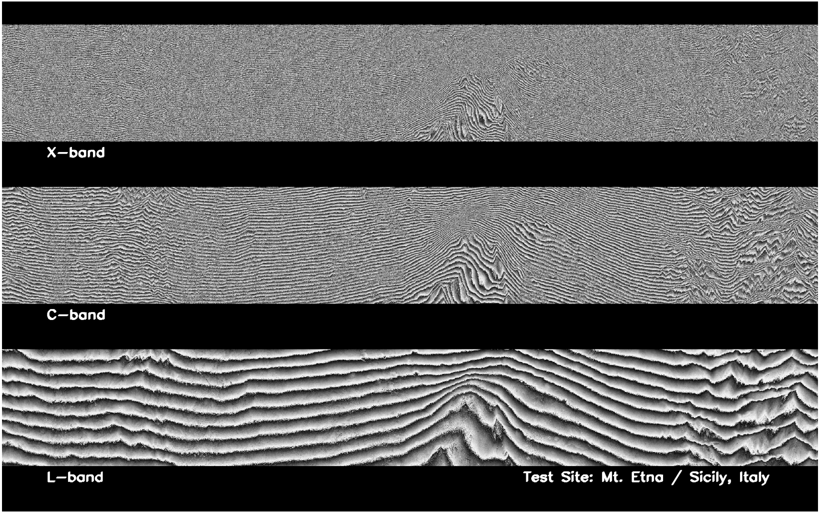

Influence of the carrier wavelength : flattened interferometric phase

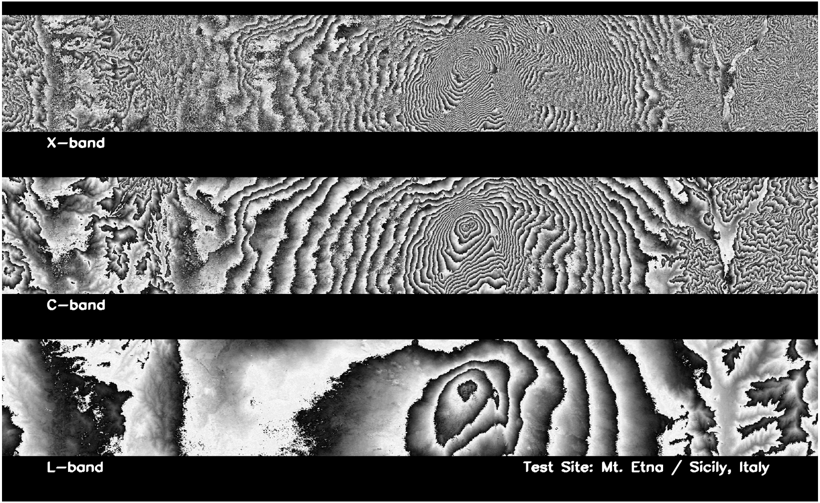

Progress

Elevation mapping using SAR images

Principles of SAR interferometry

Reconstruction of Digital Elevation Models

Principle of phase unwrapping : 1-D case

Purpose : remove discontinuous transitions. $\Delta\phi_{12\_wrapped} = \Delta\phi_{12} + k2\pi$

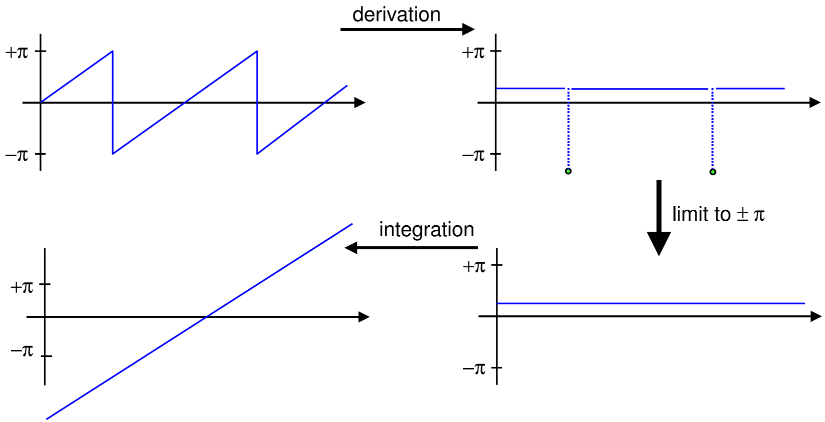

Principle of phase unwrapping : 2-D case

Example : LMSE unwrapping

- Minimize the Least Square Error between wrapped and unwrapped phase partial derivatives
- Use second order derivatives

$$\frac{\partial^2 \phi_{uw}}{\partial x^2} + \frac{\partial^2 \phi_{uw}}{\partial y^2} - \phi_w'' = 0$$

Pros and cons

- Very simple to implement
- Very fast when using FFT's
- Error propagation
- Global distorsions (Least Square)

Application

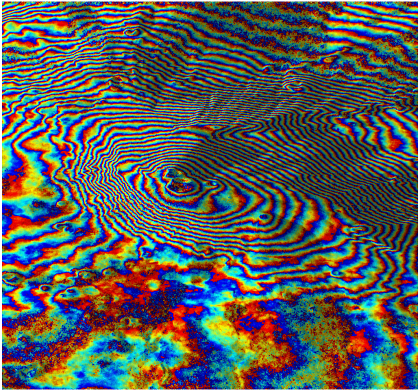

Wrapped topographic phase

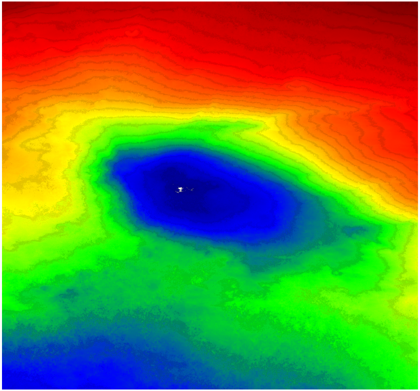

Unwrapped topographic phase

SIR-C, X-band, Mount Etna, Italy

60m baseline

Geocoding : from slant-range to cartographic coordinate systems

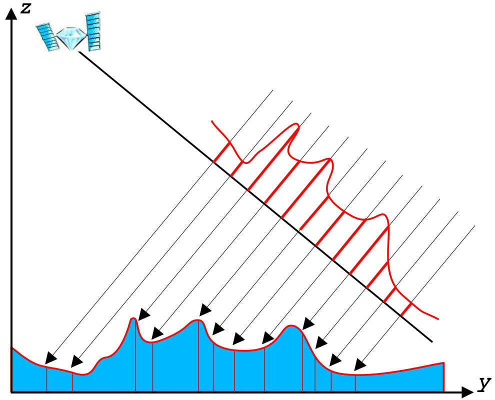

Phase to height conversion

$$\Delta\phi_{topo} = -k_c \frac{B_\perp}{r_1 \sin\theta} \Delta h$$

Slant-range to ground-range projection

- Non-linear re-sampling
- Adaptation to a coordinate system

DEM reconstruction chain

Acquired images

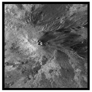

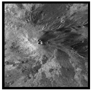

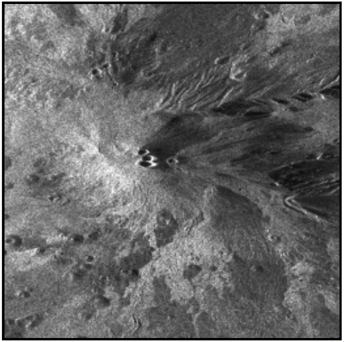

DEM reconstruction chain

Raw interferogram

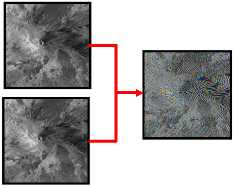

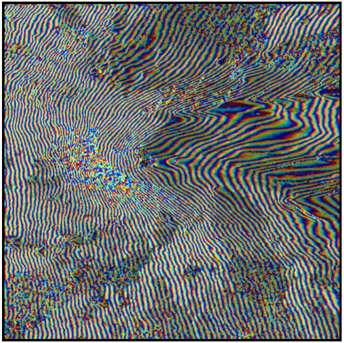

DEM reconstruction chain

Flattened interferogram

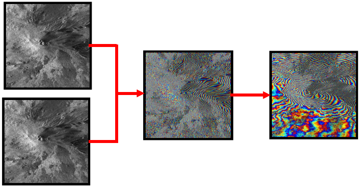

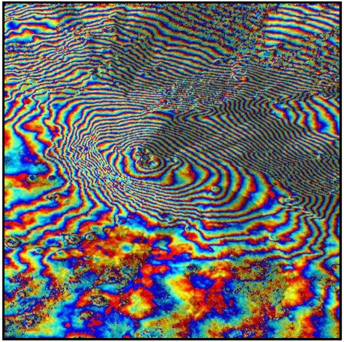

DEM reconstruction chain

Unwrapped interferogram

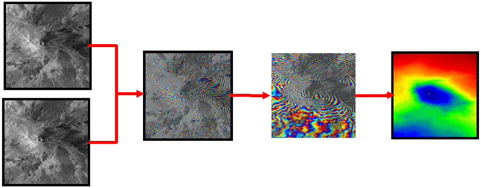

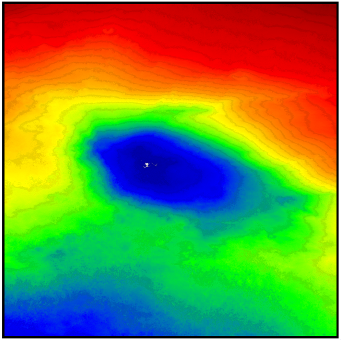

DEM reconstruction chain

Geocoded DEM

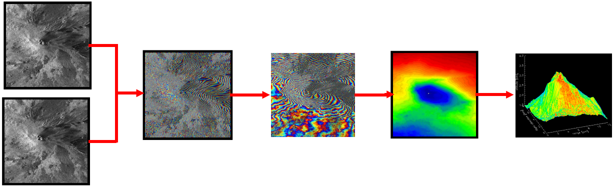

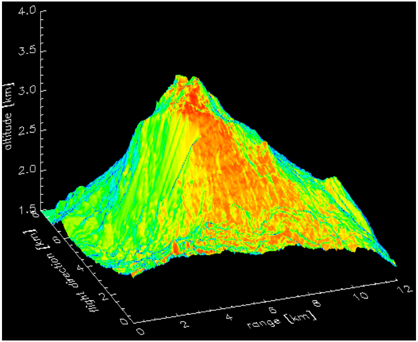

The SRTM mission

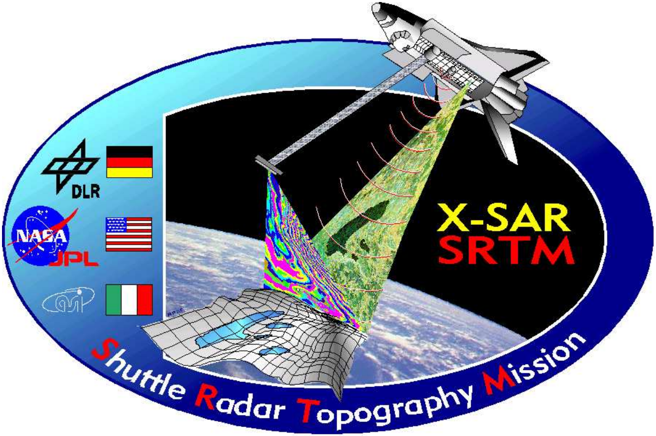

The SRTM X-SAR sensor

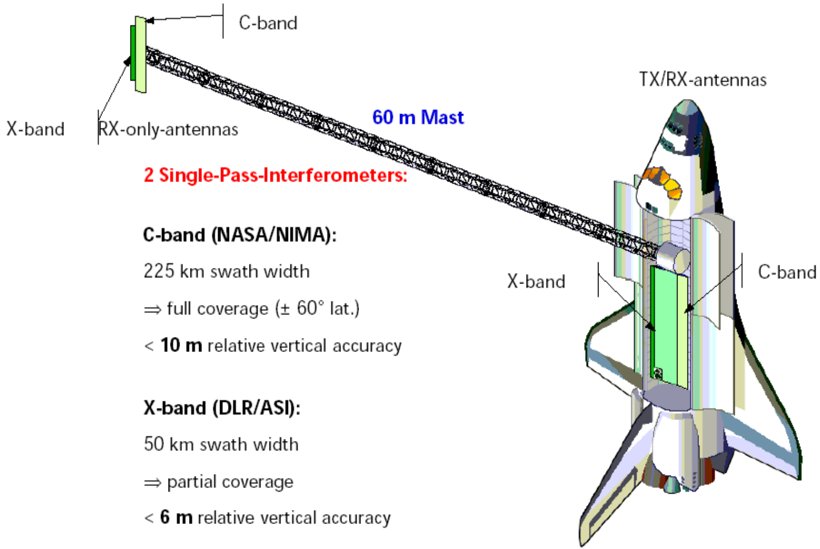

SRTM/X-SAR Image of Volcano Koma-ga-Take, Hokkaido, Japan

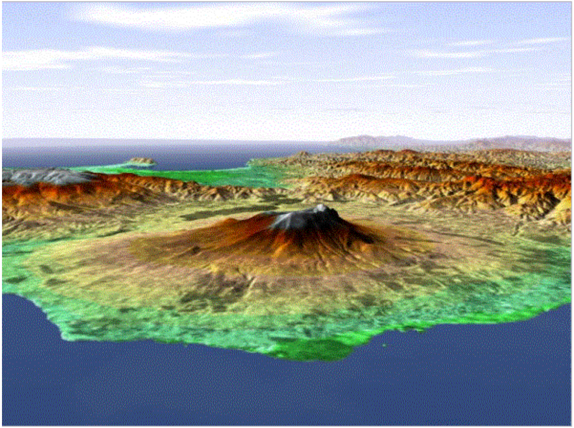

SRTM/X-SAR Image of Mount Kotopaxi, Ecuador

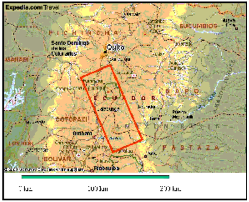

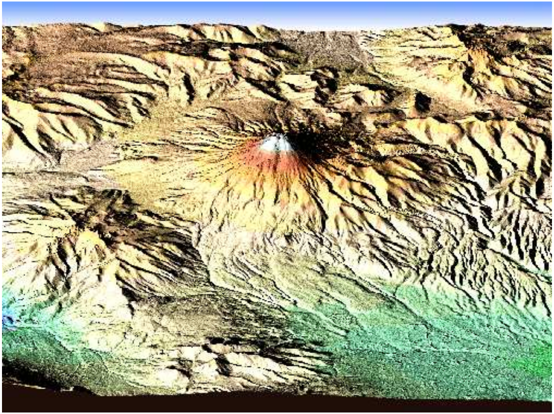

High resolution elevation mapping worldwide

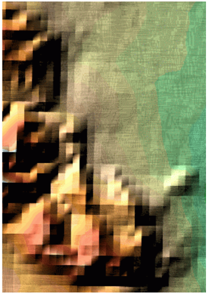

GTOP-030
Spatial Resolution: 30 Arc Sec = 1km
Height Accuracy : 100 m – 500 m

X-SAR SRTM
Shuttle Radar Topography Mission

February 2000
Single Pol Channel

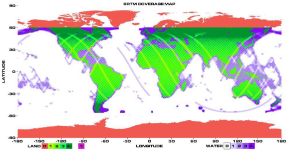

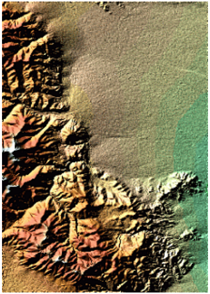

SRTM: X-SAR
Spatial Resolution: 1 Arc Sec = 30m
Height Accuracy : 6-10 m

Hydrological Water Flow Simulation : a comparison

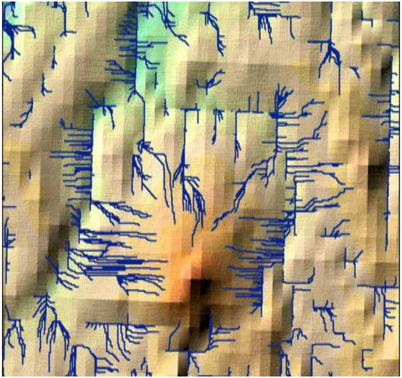

Globe-30 DEM

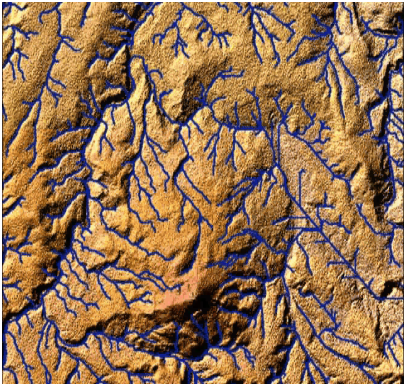

SRTM DEM

Appendix : radar-grammetry range positions

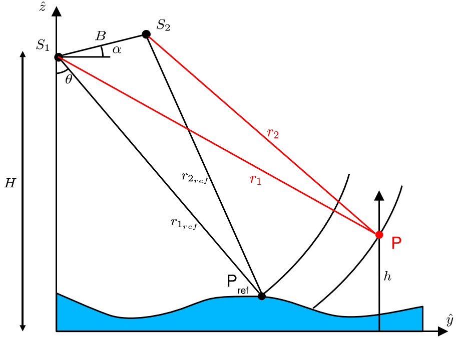

Estimation of h

$$\begin{aligned} r_2^2 = (H - h + B_v)^2 + (y_0 - B_h)^2 &= r_1^2 + B^2 + 2Br_1(\sin\alpha\cos\theta - \cos\alpha\sin\theta) \\ &= r_1^2 + B^2 - 2Br_1(\sin(\theta - \alpha)) \end{aligned}$$

with $H - h = r_1 \cos\theta, y_0 = r_1 \sin\theta,\ B_h = B\cos\theta,\ B_v = B\sin\theta$
then $h = H - r_1 \cos\theta$

Appendix : Interferometric phase, far field approximation

- From the geometry : $r_2^2 = r_1^2 + B^2 - 2Br_1 \sin(\theta - \alpha)$
- Series expansion

$$r_2 = r_1 \sqrt{1 - 2\frac{B}{r_1}(\sin(\theta - \alpha)) + \frac{B^2}{r_1^2}} = r_1 - B\sin(\theta - \alpha) + \frac{B^2}{2r_1} + \dots$$

- Approximation for $r_1 \gg B^2$: $r_2 \approx r_1 - B\sin(\theta - \alpha)$

Equivalence with a parallel plane wave approximation

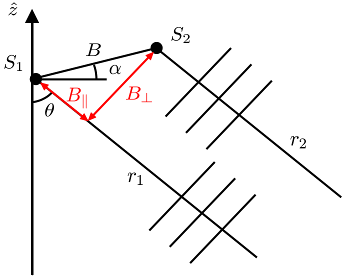

- Parallel path lengths : $r_2 = r_1 - B_\parallel$
- Parallel baseline expression : $B_\parallel = B\sin(\theta - \alpha)$

Appendix : Interferometric phase, topographic component

Topographic phase

$$\Delta\phi_{12} = -\frac{4\pi}{\lambda_c}\Delta r_{12} = k_c B \sin(\alpha - \theta) \quad , \quad \Delta\phi_{topo} = \left.\frac{\partial \Delta\phi_{12}}{\partial h}\right|_{r_1} \Delta h$$

Differentiation

$$\left.\frac{\partial \Delta\phi_{12}}{\partial h}\right|_{r_1} = \frac{\partial \Delta\phi_{12}}{\partial \theta} \left.\frac{\partial \theta}{\partial h}\right|_{r_1}$$

$$\frac{\partial \Delta\phi_{12}}{\partial \theta} = -k_c B \cos(\alpha - \theta) \quad \text{and} \quad r_1 \cos\theta = H - h \Rightarrow \left.\frac{\partial \theta}{\partial h}\right|_{r_1} = \frac{1}{r_1 \sin\theta}$$

Result

$$\Delta\phi_{topo} = \left.\frac{\partial \Delta\phi_{12}}{\partial h}\right|_{r_1} \Delta h = -k_c \frac{B \cos(\theta - \alpha)}{r_1 \sin\theta} \Delta h = -k_c \frac{B_\perp}{r_1 \sin\theta} \Delta h$$

Appendix : Interferometric phase, flat-earth component

Flat-earth phase

$$\Delta\phi_{12} = -\frac{4\pi}{\lambda_c}\Delta r_{12} = k_c B \sin(\alpha - \theta) \quad , \quad \Delta\phi_{earth} = \left.\frac{\partial \Delta\phi_{12}}{\partial r_1}\right|_h \Delta r_1$$

Differentiation

$$\left.\frac{\partial \Delta\phi_{12}}{\partial r_1}\right|_h = \frac{\partial \Delta\phi_{12}}{\partial \theta} \left.\frac{\partial \theta}{\partial r_1}\right|_h$$

$$\frac{\partial \Delta\phi_{12}}{\partial \theta} = -k_c B \cos(\alpha - \theta) \quad \text{and} \quad r_1 \cos\theta = H - h \Rightarrow \left.\frac{\partial \theta}{\partial r_1}\right|_h = \frac{1}{r_1 \tan\theta}$$

Result

$$\Delta\phi_{fe} = \left.\frac{\partial \Delta\phi_{12}}{\partial r_1}\right|_h \Delta r_1 = -k_c \frac{B\cos(\theta - \alpha)}{r_1 \tan\theta}\Delta r_1 = -k_c \frac{B_\perp}{r_1 \tan\theta}\Delta r_1$$